Dyes and Pigments 160 (2019) 671–674

Contents lists available at ScienceDirect

Dyes and Pigments

journal homepage: www.elsevier.com/locate/dyepig

The origin of slow electron injection rates for indoline dyes used in dye-sensitized solar cells

Ahmed M. El-Zohry

Department of Chemistry, Ångström Laboratories, Box 523, SE-751 20, Uppsala, Sweden

ARTICLE INFO

Keywords:
Mid-IR
Electron dynamics
Semiconductors
Torsional motions
Acceptor moities
Rhodanine
Cyano-acrylic acid

ABSTRACT

This work highlights the direct impact of selecting acceptor moiety for organic dyes on the electron dynamics at faster time scales, in which overlooked photo-physical properties are present on semiconductor surfaces with specific acceptor moieties. Four top-performing dyes of indoline family (D131, D102, D149, and D205) sharing the same donor moiety, but through different acceptor groups, were selected and compared with respect of electron injection process, using ultrafast transient-infrared probe. The presence of rhodanine moiety at the acceptor unit in D102, D149 and D205, shows an additional slow electron injection process, of picosecond time-scale, on the low band-gap semiconductor, TiO_2. This slow process is expected to be present due to a twisted intramolecular charge transfer/isomerized state of the excited dye prior to electron injection. This isomerized state reduces as well the detrimental electron recombination process rates, and results of high performance in solar cells based on these rhodanine dyes. Replacing the rhodanine moiety by a cyano-acrylic group in D131 dye shows faster electron injection and recombination processes, due to the lower dipole moment present in the excited state, hindering the formation of an isomerized state. These findings will aid to enhance the organic dyes design used in dye sensitized solar cells, in which designed photo-physical processes on semiconductor surfaces can increase the efficiencies of the solar cells.

1. Introduction

The wide-accepted strategy for building metal-free organic dyes for solar cell applications is by far connecting a donor (D) electron-rich moiety, in the ground state, through a linker unit to an acceptor (A) moiety that is electron-deficient in the ground state, which is known as push-pull strategy [1–5]. Upon light excitation, an intramolecular charge transfer (ICT) process is induced from the D to A moiety, where the electron is further transferred to the conduction band (CB) of the semiconductor [1,6,7]. To absorb most of the incident sun light, the tune of optical and electronic properties of utilized dyes occurs via changing either the D or A moieties, as well as changing the length of the linker unit [8]. Several acceptor units have been used for this aspect such as cyanoacrylic and rhodanine moieties [1,8]. These two moieties have been heavily used in various organic dyes [1,9]. Each of these moieties has its cons and pros depending on the working conditions [10]. However, the influence of acceptor unit variation has been mainly to change the spectral response of the utilized dye and/or the thermodynamic driving force between the LUMO of the excited dye and the CB, which in turn affects the photocurrent density and the open circuit voltage values in solar cells [1,9,11,12]. Very few reports have discussed the variation of kinetic parameters, more specifically electron injection and recombination, upon changing either the D or A units [6]. Nevertheless, this paper illustrates the variation of electron injection dynamics for four well-performing, metal-free, indoline dyes sharing the same D unit but with four different acceptor units, known as D131, D102, D149 and D205 (see chemical structures in Fig. 1). As can be seen in Fig. 1, D131 has a cyanoacrylic group, D102 has one rhodanine moiety, D149 has two rhodanine moieties, and D205 has additional octyl chain in top of the two rhodanine moieties. Solar cells based on D131, D102, and D149 using ZnO have shown high efficiencies among other indoline dyes, reaching to ca. 5% [13]. On TiO_2 nanorods, solar cell based on D131 has higher efficiency (ca. 5.1%), than others based on D149 and D102, which has been attributed to the highest current produced due to strong electronic coupling between the cyanoacrylic group, wherein the LUMO is located, and the TiO_2 surface [14–16]. With a development of the structural design, the long octyl-chain in D205 has led to an improvement of efficiency, 7.1%, in comparison to D149 and D102 under the same conditions due to the retardation of electron recombination process [17]. With the aid of anti-aggregation agent, efficiencies of ca. 9.5% and 9.0%, on nanocrystalline-TiO_2, could be achieved by D205 and D149, respectively [18]. It is worth mentioning that the first breakthrough of indoline dyes, which attracts the intension towards these dyes, was achieved by D149, in which an

E-mail addresses: amfzohry@yahoo.com, ahmed.elzohry@kaust.edu.sa.

https://doi.org/10.1016/j.dyepig.2018.09.002
Received 31 July 2018; Received in revised form 30 August 2018; Accepted 2 September 2018
Available online 04 September 2018
0143-7208/

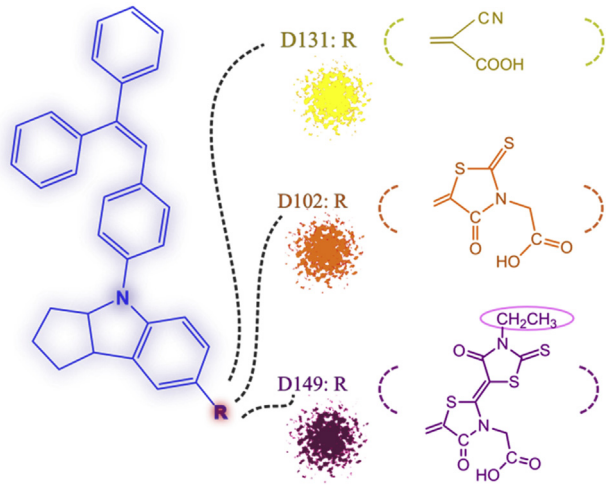

Fig. 1. Structures of indoline donor unit D (blue), and other emerging dyes D131, D102, and D149 (various colors of solid materials) with different acceptor units. The structure of D205 is similar to D149 except the presence of octyl chain instead of methyl group (surrounded by pink oval).

efficiency value of 8.2% could be obtained [19]. From the above information, one can see that efficiencies have been measured without deep understandings of the electron dynamics associated with the dye's structure. Thus, the relationship between the structure of these well-performing organic dyes and electron dynamics, mainly electron injection, will definitely improve our knowledge towards synthesizing robust dyes. To do so, the ultrafast transient absorption in the mid-infrared range (fs-IR) is used in this study to follow the electron dynamics of the selected adsorbed indoline dyes at the CB of TiO_2. The fs-IR probe has been utilized before for different systems for observing the electron injection [20–24]. The electron's transient absorption normally extends from 3333 to 11,111 nm with a broad featureless shape [25]. The fs-IR has recently shown more sensitivity towards injected electrons at the CB in semiconductors due to lack of electronic absorption from other species such as cationic organic dyes [26–28]. This unique advantage of mid-IR probe is utilized herein to follow the electron injection process for four dyes adsorbed on TiO_2, D131, D102, D149, and D205. The fs-IR dynamics show herein drastic changes in the electron dynamics upon changing the acceptor moiety for the studied dyes.

2. Results and discussion

Fig. 2A shows the normalized absorption spectra for different indoline dyes including the D unit, D131, D102 and D149 in toluene. The nature of the D's excited state is a local excited state (LE), which is changed to an intramolecular charge transfer (ICT) state upon attaching the acceptor units in the emerging dyes [16,19,29,30]. As can be seen, with increasing the acceptor unit strength, connected to the D unit ($\lambda_{max}^{abs} \approx$ 375 nm), from cyanoacrylic (D131, $\lambda_{max}^{abs} \approx$ 460 nm) till rhodanine moieties (D102 $\lambda_{max}^{abs} \approx$ 500 nm, D149 $\lambda_{max}^{abs} \approx$ 535 nm, and D205 $\lambda_{max}^{abs} \approx$ 535 nm), bathochromic shifts can be observed. These acceptor strengths were illustrated before in the theoretical work of Tangui [16], in which the dipole moment is increased by ca. a factor of two upon going from cyanoacrylic group in D131 to two rhodanine moieties in D149. These absorption spectra are broadened upon adsorption of these dyes on TiO_2, probably due to the aggregation effect, which is shown in Fig. 2B for D149 on TiO_2. Similar broadenings have been reported previously for other dyes [31–34]. However, upon using the fs-IR probe in our measurements, the aggregation problem will not influence the observed kinetics as shown previously in the visible region [32], since the working spectral region is solely sensitive to the vibrating electrons in the CB of TiO_2 [26,27].

As can be shown in Fig. 3, the adsorbed dyes on TiO_2 were excited in the visible region by 410 nm, and probed in the mid-IR region at 4900 nm, where the signature of the electron dynamics in the CB in TiO_2 can be followed, different kinetic profiles can be observed depending on the dye structure. At time zero, the signal of injected electrons at 4900 nm is produced, representing the electron transfer process from the excited dye to the CB of TiO_2, see Fig. 3. Beyond time zero, slow injection time constants can be detected for D102, D149 and D205, except D131. Later on, the signal starts to decay due to the electron recombination process between electrons in the CB of TiO_2 to the nearby oxidized dyes on surface, however, the full recovery of electrons is beyond our time window of the current measurements, ca. 5 ns. Therefore, accurate analysis for electron recombination process has not been performed. Table 1 summarizes the time constants obtained from fitting the kinetic traces using multi-exponential components. To the best of current knowledge, the slow electron injection time constant, in the order of ps time scale, was rarely observed for organic dyes, and not fully understood [6]. Even for the D149 dye that has been heavily studied spectroscopically on semiconductors, only electron injection components of 100–250 fs were observed [35–37]. Most likely, the slow injection process was not observed due to the usage of visible probe to detect this crucial process, in which an overlap between signals of electron absorption, oxidized dye and excited state of non-injecting dyes on surfaces, making the data analysis quite challenging. Nevertheless, previously, the electron injection process of D149 in complete solar cell probed by mid-IR spectrum exhibited similar results to the ones in this work [23].

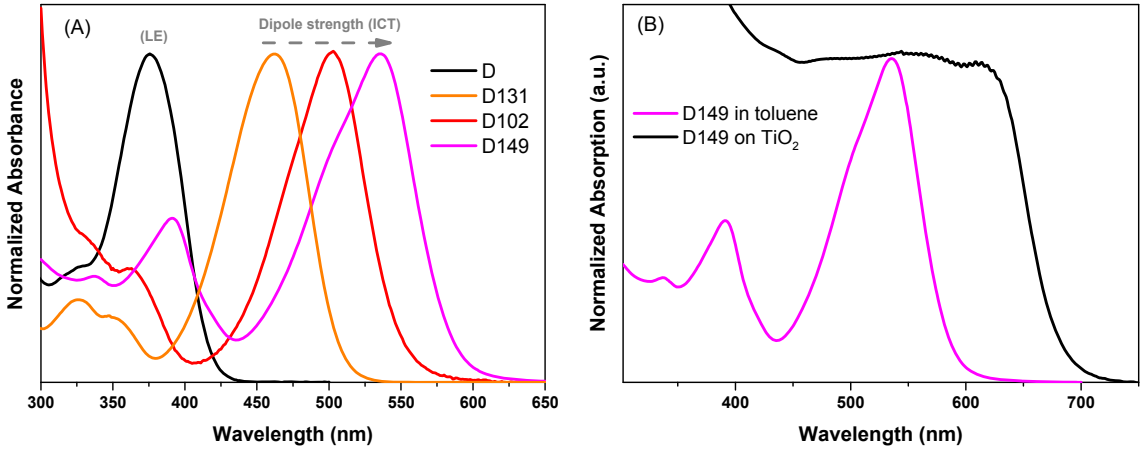

Fig. 2. (A) Normalized absorption spectra of the D unit and different dyes studied of the indoline family (D131, D102, and D149) in toluene. (B) Comparison between D149 in toluene and upon adsorption on TiO2. Check text for more information.

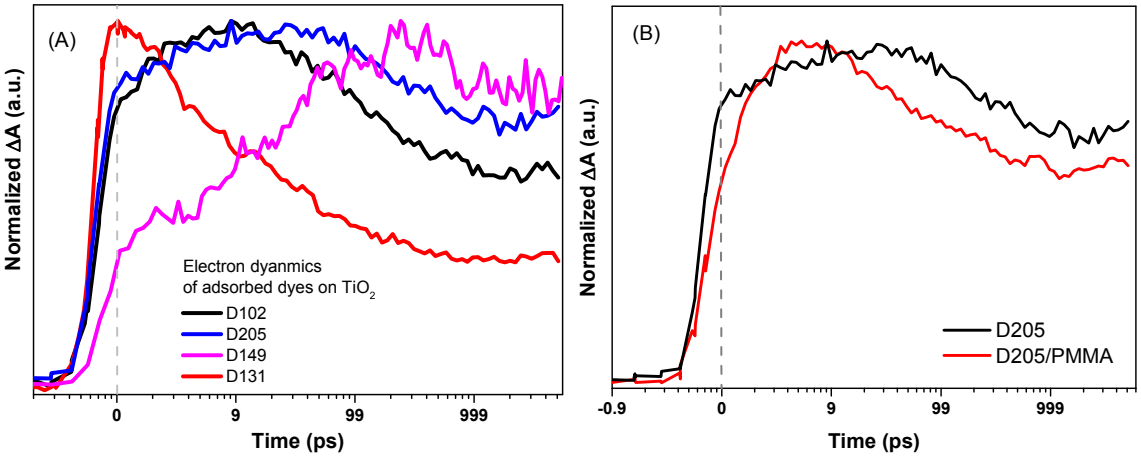

Fig. 3. (A) Normalized kinetic traces extracted from the fs-TA in the infrared region for the electron injection process from different dyes, shown in different colors, on TiO_2. The excitation wavelength was 410 nm and the probe wavelength was 4900 nm. (B) Comparison between kinetic traces for the electron dynamics of adsorbed D205 on TiO_2 in the absence and presence of PMMA. (For interpretation of the references to color in this figure legend, the reader is referred to the Web version of this article.)

Table 1
Time constants for electron injection process from various indoline dyes on TiO_2. Times are shown in picosecond with corresponding amplitudes in percent between parentheses.

Dye	τ_1 (%)	τ_2 (%)
D131	0.15 (100)	
D102	0.24 (76)	1.73 (24)
D149	0.45 (50)	30 (50)
D205	0.32 (91)	9.1 (9)
D205/PMMA	0.7 (100)	

All the fitting data show bi-exponential behavior for the investigated dyes except the D131 dye, only one exponential lifetime is used (Table 1). Apparently, all the dyes with rhodanine moiety (D102, D149, and D205) show slower electron injection components of ps, and upon replacing this rhodanine moiety by cyanoacrylic group, in D131, only a fast injection component of 150 fs is shown (Table 1). Seemingly, the value of the second injection time constant rises with the number of rhodanine moieties present, D149 > D102 (Table 1). More illustratively, D102, with one rhodanine moiety, has a second time constant of ca. 1.7 ps, and for D149, with two rhodanine moieties, it has a component of 30 ps with high amplitude of 50% (Table 1). However, for D205 that is similar to D149 (see Fig. 1), the second injection time constant is lower than in D149, although they share the same number of rhodanine moieties, this can be attributed to the presence of additional long alkyl chain in D205, hindering some torsional motions in the excited state (Fig. 1). It is expected that the presence of the second slow electron injection component in D102, D149, and D205 is due to the strong acceptor group offered by rhodanine moiety that is stronger than cyanoacrylic unit, in D131 [16]. The existence of a strong acceptor group can lead to a twisted intramolecular charge transfer (TICT)/isomerized state on semiconductor surfaces, which in turn can lead to a slow injection process and slow recombination process due to the weak coupling between the twisted cationic dye and the CB vibrational levels on TiO_2 [26,38,39]. To confirm the existence of TICT/isomerized state on TiO_2, harsh theoretical calculations are needed to be done, which are currently under-construction. However, to confirm the contribution of large-scale motions on semiconductor surfaces by a simple experimental trick, a layer of PMMA polymer was physically distributed over the adsorbed D205 on TiO_2. PMMA is known to hinder observed large-scale motions of dyes and molecules in solutions [32]. Upon using PMMA, the electron injection profile has been significantly changed, in which the average injection lifetime for D205/TiO_2 is ca. 1.2 ps that is becoming faster to 0.7 ps upon using the PMMA on top of the D205 film (Fig. 3B and Table 1). These changes in electron injection rates upon using PMMA confirms the existence of large-scale motions of adsorbed dyes prior to injection process. The presence of TICT state or an isomerized state on semiconductor surfaces have been discussed and illustrated before for other organic dyes [26,29,32,38,40,41]. More importantly, the presence of TICT/isomerized injection state leads to slower electron recombination process [26,38,41]. This is also shown in Fig. 3B, in which for the same amount of injected electrons (normalized kinetics), the electron recombination is faster for D131 than other dyes with the rhodanine moieties due to the strong coupling between the ICT of cationic D131 and the CB of TiO_2. As shown in Fig. 3, for the same amount of injected electrons, electron recombination for D149 and D205 are very similar in the current time window, which can illustrate the similar performance of the two dyes under standard conditions [18]. For instance, solar cells based on both dyes, D149 and D205, showed similar efficiencies of 8.2% and 8.4%, respectively [18]. Although the octyl chain, in D205, reduces the amount of electron being injected from the TICT/isomerized state due to slower amplitudes of the slow electron injection components (Table 1), the octyl chain is still significant to reduce the aggregation present on semiconductor surfaces and show high performance in solar cells [18]. Therefore, on top of the known properties for the rhodanine as a strong acceptor group that shifts the absorption spectrum of the adsorbed dye towards the IR region allowing the dye to absorb more photons, it can also induce the formation of TICT/isomerized state that has direct impact on the electron injection and recombination processes.

3. Conclusions

In summary, the comparison of electron dynamics using sensitive mid-IR probe, more specifically, the electron injection process, for the well-known indoline dyes, D131, D102, D149 and D205, reveals slow electron injection trend for dyes having the rhodanine moiety. This slow injection process is likely due to the formation of TICT/isomerized state, which has a direct impact as well on the electron recombination process and the performance of these dyes in solar cells as shown previously [19,30,42,43]. Also, contrary to the traditional view that ultrafast electron injection rates for dyes used in solar cells dominate the whole kinetics, the slow injection rates can contribute as well to the high efficiencies in solar cells based on such dyes. Finally, this letter paves the way towards smarter design for organic dyes taking into account the overlooked photo-physical processes occurring on semiconductor surfaces.

4. Material and methods

4.1. Steady state measurements

Absorption spectra were measured on a Varian Cary 5000.

4.2. Ultrafast transient measurements

The detailed specifications of the instrumentation have been described earlier [28]. Briefly, excitation wavelength of 410 nm was employed when using the fs-infrared (IR) probe centralized at 4900 nm. The average excitation power ranged from 200 to 350 mW. All the obtained data were background corrected. Extracting the lifetimes from the kinetic traces are based on using multi-exponential decays equations.

4.3. Substances

All the used indoline dyes were obtained as a kind gift from Masakazu Takata, Mitsubishi Paper Mills, and used as received. Plastic fragments of PMMA (ca. 1 − 5 mm in diameter) were dissolved in $CHCl_3$ and the solution used for doctor blading of polymer films as described previously [32]. The sensitization of indoline dyes on TiO_2 films, made by doctor blading, carried by CaF_2 films for ultrafast IR measurements. More details about the preparation of TiO_2 have been illustrated previously [28].

Acknowledgements

Thanks for Prof. Leif Hammarström for providing the necessary tools to do these measurements in his lab at UU, Sweden. Lots of thanks to Masakazu Takata for kindly sending a sample of indoline dyes (Japan). Many thanks for Dr. Burkhard Zietz for his highly valuable scientific and technical support all the time at UU, Sweden.

References

[1] Liang M, Chen J. Chem Soc Rev 2013;42:3453.
[2] Babu DD, Cheema H, Elsherbiny D, El-Shafei A, Adhikari AV. Electrochim Acta 2015;176:868–79.
[3] Babu DD, Gachumale SR, Anandan S, Adhikari AV. Dyes Pigments 2015;112:183–91.
[4] Naik P, Su R, Elmorsy MR, Babu DD, El-Shafei A, Adhikari AV. J Photochem Photobiol, A 2017;345:63–73.
[5] Babu DD, Su R, El-Shafei A, Adhikari AV. Electrochim Acta 2016;198:10–21.
[6] Furube A, Katoh R, Hara K. Surf Sci Rep 2014;69(4):389–441.
[7] Babu DD, Su R, Naik P, El-Shafei A, Adhikari AV. Dyes Pigments 2017;141:112–20.
[8] Clifford JN, Martinez-Ferrero E, Viterisi A, Palomares E. Chem Soc Rev 2011;40(3):1635–46.
[9] Hagfeldt A, Boschloo G, Sun LC, Kloo L, Pettersson H. Chem Rev 2010;110(11):6595–663.
[10] Chen C, Yang XC, Cheng M, Zhang FG, Sun LC. Chemsuschem 2013;6(7):1270–5.
[11] Babu DD, Su R, El-Shafei A, Adhikari AV. RSC Adv 2016;6(36):30205–16.
[12] Babu DD, Elsherbiny D, Cheema H, El-Shafei A, Adhikari AV. Dyes Pigments 2016;132:316–28.
[13] Dentani T, Kubota Y, Funabiki K, Jin J, Yoshida T, Minoura H, Miura H, Matsui M. New J Chem 2009;33(1):93–101.
[14] Jose R, Kumar A, Thavasi V, Fujihara K, Uchida S, Ramakrishna S. Appl Phys Lett 2008;93(2).
[15] Jose R, Kumar A, Thavasi V, Ramakrishna S. Nanotechnology 2008;19(42).
[16] Le Bahers T, Pauporte T, Scalmani G, Adamo C, Ciofini I. Phys Chem Chem Phys 2009;11(47):11276–84.
[17] Kuang D, Uchida S, Humphry-Baker R, Zakeeruddin SM, Gratzel M. Angew Chem Int Ed 2008;47(10):1923–7.
[18] Ito S, Miura H, Uchida S, Takata M, Sumioka K, Liska P, Comte P, Pechy P, Grätzel M. Chem Commun (J Chem Soc Sect D) 2008;41:5194–6.
[19] Horiuchi T, Miura H, Sumioka K, Uchida S. J Am Chem Soc 2004;126(39):12218–9.
[20] Asbury JB, Ellingson RJ, Ghosh HN, Ferrere S, Nozik AJ, Lian TQ. J Phys Chem B 1999;103(16):3110–9.
[21] Furube A, Du L, Hara K, Katoh R, Tachiya M. J Am Chem Soc 2007;129(48):14852–5.
[22] Furube A, Murai M, Watanabe S, Hara K, Katoh R, Tachiya M. J Photochem Photobiol, A 2006;182(3):273–9.
[23] Juozapavicius M, Kaucikas M, van Thor JJ, O'Regan BC. J Phys Chem C 2012;117(1):116–23.
[24] Juozapavicius M, Kaucikas M, Dimitrov SD, Barnes PRF, van Thor JJ, O'Regan BC. J Phys Chem C 2013;117(48):25317–24.
[25] Yamakata A, Ishibashi T, Onishi H. Chem Phys Lett 2001;333(3–4):271–7.
[26] El-Zohry AM, Cong J, Karlsson M, Kloo L, Zietz B. Dyes Pigments 2016;132:360–8.
[27] Abdellah M, El-Zohry AM, Antila LJ, Windle CD, Reisner E, Hammarström L. J Am Chem Soc 2017;139(3):1226–32.
[28] Antila LJ, Santomauro FG, Hammarström L, Fernandes DL, Sá J. Chem Commun (J Chem Soc Sect D) 2015;51(54):10914–6.
[29] El-Zohry AM, Roca-Sanjuan D, Zietz B. J Phys Chem C 2015;119(5):2249–59.
[30] Horiuchi T, Miura H, Uchida S. Chem Commun (J Chem Soc Sect D) 2003;24:3036–7.
[31] Feng S, Li QS, Sun PP, Niehaus TA, Li ZS. ACS Appl Mater Interfaces 2015;7(40):22504–14.
[32] El-Zohry A, Orthaber A, Zietz B. J Phys Chem C 2012;116(50):26144–53.
[33] Sakuragi Y, Wang XF, Miura H, Matsui M, Yoshida T. J Photochem Photobiol, A 2010;216(1):1–7.
[34] Pastore M, Angelis FD. ACS Nano 2010;4(1):556–62.
[35] Fakis M, Stathatos E, Tsigaridas G, Giannetas V, Persephonis P. J Phys Chem C 2011;115(27):13429–37.
[36] Oum K, Lohse PW, Flender O, Klein JR, Scholz M, Lenzer T, Du J, Oekermann T. Phys Chem Chem Phys 2012;14(44):15429–37.
[37] Rohwer E, Richter C, Heming N, Strauch K, Litwinski C, Nyokong T, Schlettwein D, Schwoerer H. ChemPhysChem 2013;14(1):132–9.
[38] Debnath T, Maity P, Lobo H, Singh B, Shankarling GS, Ghosh HN. Chem Eur J 2014;20(12):3510–9.
[39] Rettig W. Angew Chem Int Ed 1986;25(11):971–88.
[40] Zietz B, Gabrielsson E, Johansson V, El-Zohry AM, Sun L, Kloo L. Phys Chem Chem Phys 2014;16(6):2251–5.
[41] El-Zohry AM. Exploring organic dyes for grätzel cells using time-resolved spectroscopy PhD. Thesis Uppsala University; 2015.
[42] Kim JY, Kim YH, Kim YS. Curr Appl Phys 2011;11(1):S117–21.
[43] Matsui M, Asamura Y, Kubota Y, Funabiki K, Jin JY, Yoshida T, Miura H. Tetrahedron 2010;66(37):7405–10.